

RAPID COMMUNICATION

Inge Højgaard · Anne-Marie Fornander
Mari-Anne Nilsson · Hans-Göran Tiselius

Crystallization during volume reduction of solutions with a composition corresponding to that in the collecting duct: the influence of hydroxyapatite seed crystals and urinary macromolecules

Received: 8 July 1998 / Accepted: 12 March 1999

Abstract To examine the effect of hydroxyapatite (HAP) seed crystals and urinary macromolecules on the crystallization under conditions similar to those in the collecting duct, we evaporated 100 ml samples of salt solutions with an ion composition assumed to correspond to that in the collecting duct without and with HAP seed crystals. The crystallization in seeded solutions was assessed both with and without dialysed urine (dU). After evaporation the number and volume of crystals were recorded in a Coulter Multisizer and the crystal morphology examined with scanning electron microscopy (SEM) and X-ray crystallography. Addition of HAP crystals was apparently followed by an approximately 15–20% increase in heterogeneous nucleation of calcium oxalate (CaOx). In these experiments SEM and X-ray crystallography showed a high percentage of CaOx in the precipitate. In samples reduced to 40–69 ml, addition of dU to the collecting duct solution containing HAP seed resulted in a greater mean (SD) number of crystals; 3895 (1841) in samples with dU and 1785 (583) in samples without. This was mainly explained by an increased mean (SD) number of small crystals. The mean crystal volume was 17.8 (1.1) and 34.3 (9.1) in samples reduced to 40–69 ml with and without dU, respectively. This might reflect the inhibitory effect of dU on the growth and/or aggregation of the CaOx-CaP precipitate or a promoted nucleation resulting in a large number of small crystals. It is concluded that calcium phosphate formed above the collecting duct might induce heterogeneous nucleation of CaOx at lower levels of the renal collecting system, and that urinary macromolecules are powerful modifiers of these processes.

Key words Crystallization · Hydroxyapatite · Calcium phosphate · Calcium oxalate · Collecting duct · Macromolecules · Promotion · Inhibition

Introduction

The mechanisms of formation of urinary calcium oxalate (CaOx)-containing concrements are incompletely understood, and the process can certainly not be explained by a crystallization of CaOx alone. Urinary stones have an organic matrix accounting for approximately 2.5% of their weight [10]. It has also been shown that a considerable fraction of CaOx stones is composed of mixtures of CaOx and calcium phosphate (CaP) [28, 29, 40, 41, 45, 46, 52]. Furthermore Leusmann and coworkers [30] showed that more than 70% of oxalate-rich stones had CaP within or near their central core.

It is reasonable to assume that the crystallization is initiated in the nephron [3, 12, 14, 18, 19, 26, 34, 54]. Finlayson and Reid [15] showed that even with a maximal crystal growth of CaOx the renal transit time was too short to result in crystals with a size that would obstruct the collecting duct. Baumann and coworkers [4] showed that after an oral oxalate load the size of the crystals was generally smaller than 200 μm in a concentrated overnight urine. In a recent experimental study Kok and Khan [25], however, concluded that during the normal transit time for urine through the nephron crystalline particles might form large enough to be retained, mainly due to the size-increasing effect of agglomeration. Thus a pronounced agglomeration and crystal retention are factors that might be of importance for stone development. Randall's plaques seem to start from a CaP deposition in the papillary tissue [47] and it has been shown that crystals of hydroxyapatite can induce a heterogeneous crystallization of CaOx [6, 7, 16, 17, 51]. Crystals of CaP that are retained in the nephron or in the renal collecting system are therefore highly interesting as possible promoters of CaOx nucleation.

I. Højgaard (✉)
Department of Surgery, Västervik Hospital,
593 81 Västervik, Sweden

A.-M. Fornander · M.-A. Nilsson · H.-G. Tiselius
Department of Biomedicine and Surgery,
Division of Urology and the Clinical Research Center,
Faculty of Health Sciences, University Hospital,
581 85 Linköping, Sweden

In two recent studies [18, 34] we have shown that there is a risk of CaP crystal formation in the proximal and distal tubule whereas CaOx is the primary type of crystal that forms in the collecting duct. In a recent study Kok [26] also found that crystallization of CaOx is most likely in the collecting duct, and it has been shown by several authors that there is a high risk of CaP crystallization at a nephron level above the collecting duct [3, 12, 26]. These observations have raised the question of whether CaP formed at a high level in the nephron is a natural and common promoter of CaOx nucleation in the collecting duct. Heterogeneous crystallization of CaOx induced by CaP is a mechanism that has previously been proposed by several authors [2, 5, 7, 22, 27, 35, 36, 43, 44].

The aim of this study was to examine whether CaP crystals can induce heterogeneous nucleation of CaOx under conditions corresponding to those in the collecting duct and to study the possible influence of the urinary macromolecules on this process. Since hydroxyapatite (HAP) is the thermodynamically most stable form of CaP [13], HAP crystals were used in these experiments.

Materials and methods

Salt solutions with an ion composition assumed to correspond to that of urine in the distal part of the collecting duct were prepared by dissolving in Millipore-filtered water as previously described [34] the following commercially available salts: calcium chloride ($\text{CaCl}_2 \times 2\text{H}_2\text{O}$), magnesium chloride ($\text{MgCl}_2 \times 6\text{H}_2\text{O}$), sodium chloride (NaCl), potassium chloride (KCl), sodium sulphate (Na_2SO_4), sodium phosphate (Na_2HPO_4), sodium oxalate ($\text{C}_2\text{Na}_2\text{O}_4$) and sodium citrate ($\text{C}_6\text{H}_5\text{Na}_3\text{O}_7 \times 2\text{H}_2\text{O}$). One litre of this solution was given the following ion composition: calcium 4.50 mmol, magnesium 3.85 mmol, phosphate 32.3 mmol, oxalate 0.32 mmol, citrate 3.21 mmol, sodium 106 mmol, potassium 63.7 mmol and sulphate 20.8 mmol. No ammonium was added to avoid the risk of precipitating ammonium salts. The pH was set to 5.80, which was considered the average pH in the collecting duct according to the results reported by Rector [48].

A suspension of HAP seed crystals with a concentration of 400 $\mu\text{g}/\text{ml}$ was prepared by adding the commercially available salt (Merck, Darmstadt, Germany) to Millipore-filtered water. After ultrasonication for 30 min the crystal size distribution was analysed in a Coulter Multisizer (Coulter Electronic, Luton, UK). No crystals were found with a size greater than 15.4 μm and the size distribution showed that 93% of the crystals had a diameter of 2.4–4.4 μm , 5% a diameter of 4.5–5.4 μm and 2% a diameter of 5.5–15.4 μm . Scanning electron microscopy of the suspension showed that the majority of the crystals were smaller than 2.4 μm and that the fractions found in a different size interval were composed of HAP crystal aggregates (Fig. 1).

Pooled dialysed bladder urine (dU) from 10 normal male subjects was used as a source of macromolecules, thereby ignoring the fact that certain macromolecules might have been added to the urine as a result of its passage and storage in the lower parts of the urinary system whereas others might have been removed during the preparation of dU. This urine was collected between 2200 and 0600 hours, and screened to exclude bacteria, protein and glucose before being pooled. Urine was dialysed as previously described [34]. According to the concentration of urine in the distal part of the collect duct, the samples with dU were prepared by dissolving the necessary salts in the dU.

Solution samples of 100 ml were passed through Millipore filters with a pore size of 0.22 μm (Millipore, Molsheim, France)

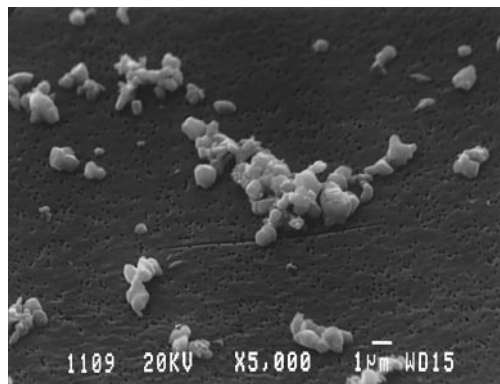


Fig. 1 Scanning electron microscopic examination of hydroxyapatite (HAP) seed crystals in a concentration of 400 $\mu\text{g}/\text{ml}$. The precipitate is shown at a magnification of $\times 5000$

before evaporation in a Büchi Rotavapor RE at 37°C (Büchi, Flawil, Switzerland). The filtration was carried out at room temperature at a rate of approximately 1 ml/s. Evaporation was performed of salt solutions without either HAP and dU (CD solution), of salt solutions with 1 ml of HAP suspension but without dU (CD-HAP solution) and of salt solutions with 1 ml of HAP suspension and with dU (CD-HAPdU solution). After evaporation to a predetermined volume, the number and volume of crystals in the size interval 2.4–45 μm were recorded in a Coulter Multisizer with a 100 μm capillary tube, which we have found most appropriate for assessing crystals in this interval. Furthermore the distribution of the crystals was recorded in the following size intervals: 2.4–5.1 μm , 5.1–10.2 μm , 10.2–20.2 μm and 20.2–45 μm . Recordings were carried out both immediately after evaporation and after 60 min of continuous agitation in an incubator at 37°C. The mean crystal volume (MCV) was calculated as the quotient between the total volume (μm^3) and the total number of crystals. After evaporation the mean and standard deviation (SD) were calculated for the following sample volume intervals: 70–95 ml (sample A), 40–69 ml (sample B) and 10–39 ml. No sample was reduced to less than 10% of its original volume.

The ion-activity products of CaOx (AP_{CaOx}), calcium hydrogen phosphate, brushite (AP_{Bru}), hydroxyapatite (AP_{HAP}), amorphous calcium phosphate (AP_{ACP}) and octacalcium phosphate (AP_{OCP}) at different degrees of evaporation, were calculated by means of computerized iterative approximation with the EQUIL2 program [57]. For ACP, we used the approximate formula $\text{Ca}(\text{PO}_4)_{0.74}(\text{H})_{0.22}$ [13].

The crystal morphology was studied in a JEOL JSM-840 scanning electron microscope (Tokyo, Japan). Preparation for scanning electron microscopy (SEM) was performed as described in detail previously [34].

Solutions CD, CD-HAP and CD-HAPdU were evaporated down to a volume of 70–80 ml, 40–50 ml and 10–20 ml. Half the crystalline material recovered from these samples was pooled before being centrifuged at 1500 rpm for 15 min. The other half was left for 60 min of continuous agitation in an incubator at 37°C before being pooled and centrifuged at 1500 rpm for 15 min. The sediment was dried in air and then subjected to X-ray crystallographic examination at LC Herring and Company (Orlando, Fla., USA) for quantitative assessment of the content of CaOx and CaP.

Statistical analysis

Wilcoxon's rank sum test was used for comparing samples with and without HAP, and with and without dU. Wilcoxon's signed rank test was used to compare samples immediately after evaporation with those obtained after 60 min of continuous agitation in the incubator.

Results

Scanning electron microscopy showed that volume reduction of the CD solution resulted in formation of CaOx and CaP crystals. Thus CaOx dihydrate (COD) was the predominant crystal phase in the least concentrated samples immediately after evaporation (Fig. 2A) whereas CaP became more common in samples subjected to more excessive volume reduction (Fig. 2E). CaP predominated in samples drawn after 60 min irrespective of the degree of volume reduction (Fig. 2B, D, F). These findings were supported by analysis with X-ray crystallography (Table 1) showing that the precipitate obtained from the CD solution immediately after evaporation contained 50% COD, 40% brushite and 10% HAP following a volume reduction to 70–80 ml, and 35% COD, 60% brushite and 5% HAP when the volume was reduced to 40–50 ml. The dominance of

CaP, mainly as brushite, was even more pronounced with further volume reduction.

During the 60 min following evaporation of the CD solutions, the crystal number and volume in sample A did not change (Table 2). In contrast these variables increased significantly with the more extensive volume reduction in sample B.

As a result of the presence of seed crystals a larger number of crystals as well as greater crystal volumes were recorded in the CD-HAP solutions in comparison with the CD solutions immediately after evaporation in both samples A and B (Table 2). As expected this difference was mainly seen in the size interval 2.4–5.1 μm . In comparison with the CD solution, samples A and B from the CD-HAP solutions had a lower MCV both immediately after evaporation and 60 min later (Table 2). In addition to the added HAP seed in the CD-HAP solutions, the larger number of crystals in samples A and B could probably be explained by the

Fig. 2A–F Scanning electron microscopic examination of the precipitate after evaporation of 100 ml samples of CD solution. **A, B** Evaporated down to a final volume of 70–80 ml, **A** immediately after evaporation and **B** 60 min after evaporation. **C, D** Evaporated down to a final volume of 40–50 ml, **C** immediately after evaporation and **D** 60 min after evaporation. **E, F** Evaporated down to a final volume of 10–20 ml, **E** immediately after evaporation and **F** 60 min after evaporation. The precipitate is shown at a magnification of $\times 1000$

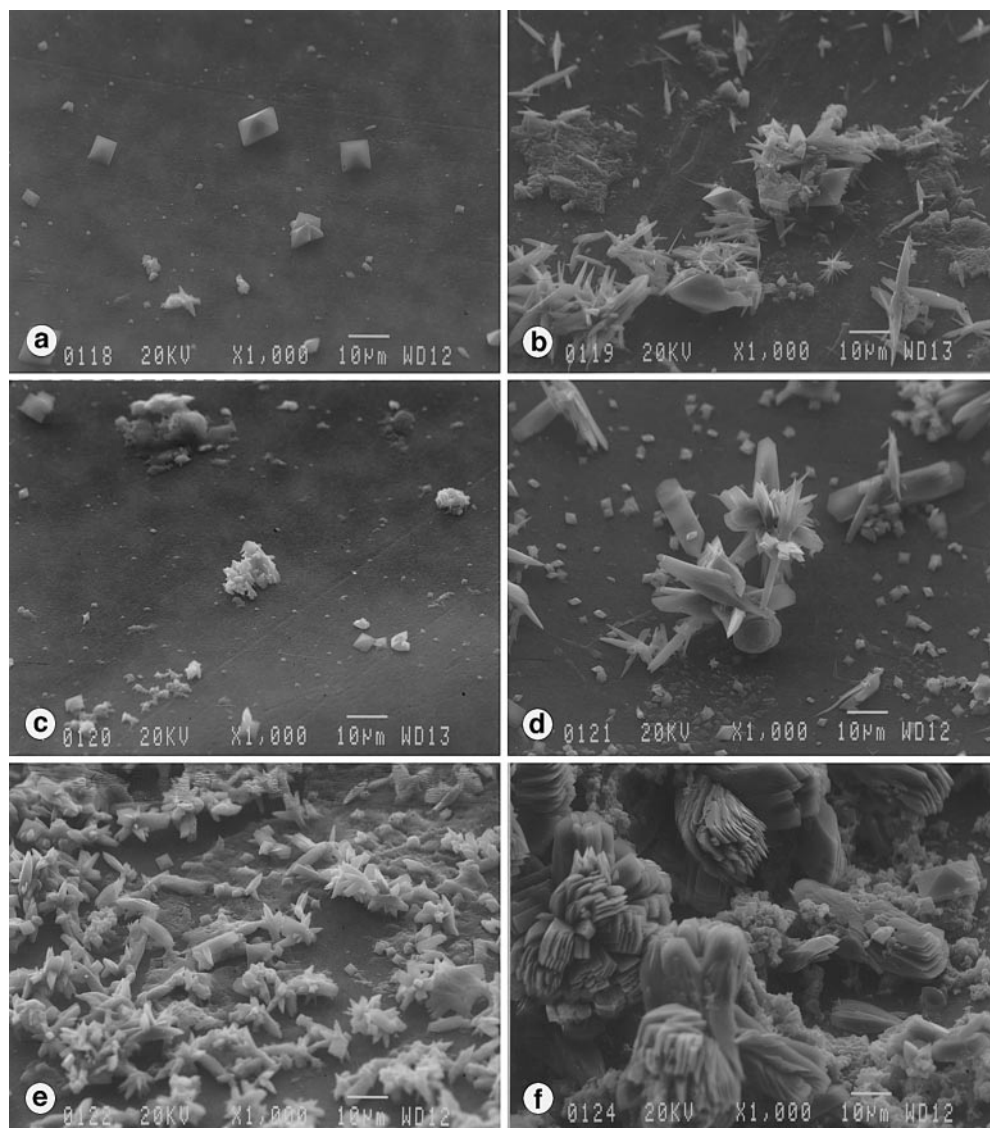


Table 1 The percentage of different calcium salts in the precipitate at different degrees of evaporation of 100 ml samples of CD, CD-HAP and CD-HAPdU solutions analysed by X-ray crystallography (*COD* calcium oxalate dihydrate, *COM* calcium oxalate monohydrate, *Bru* brushite, *HAP* hydroxyapatite, *CaOx* calcium oxalate, *CaP* calcium phosphate)

Sample volume after evaporation (ml)	Salt solution	Time (min)	Percentage of calcium salt in the sample					
			COD	COM	Bru	HAP	Total CaOx	Total CaP
70–80	CD	0	50	0	40	10	50	50
		60	35	0	55	10	35	65
	HAP	0	45	20	5	30	65	35
		60	15	45	5	35	60	40
	HAP-CDdU	0	35	0	5	60	35	65
		60	20	0	5	75	20	80
40–50	CD	0	35	0	60	5	35	65
		60	20	0	65	15	20	80
	HAP	0	50	5	10	35	55	45
		60	40	0	50	10	40	60
	HAP-CDdU	0	60	0	5	35	60	40
		60	35	0	5	60	35	65
10–20	CD	0	10	0	70	20	10	90
		60	5	0	90	5	5	95
	HAP	0	30	0	40	30	30	70
		60	20	0	70	10	20	80
	HAP-CDdU	0	20	0	75	5	20	80
		60	5	5	85	5	10	90

Table 2 Mean (SD) number, total crystal volume and mean crystal volume (MCV) at different sample volumes immediately and 60 min after evaporation of 100 ml samples of CD, CD-HAP and CD-HAPdU-solutions (crystal size 2.4–45 μm)

	Time (min)	Sample A (70–95 ml)			Sample B (40–69 ml)		
		CD	CD-HAP	CD-HAPdU	CD	CD-HAP	CD-HAPdU
No. of crystals	0	131 (133) ^{††}	1372 (378) [°]	1479 (588)	347 (315) ^{††°}	1785 (533) [°]	3895 (1841) ^{**°}
	60	127 (142)	926 (232) [°]	1414 (755)	1999 (1476) ^{††°}	2659 (1089) [°]	5398 (2254) [°]
Total crystal volume (1000 $\times \mu\text{m}^3$)	0	30.4 (41.0)	54.3 (26.6)	61.6 (42.3)	30.2 (31.5) ^{†°}	59.9 (19.3) [°]	134 (50.9) ^{**°}
	60	27.0 (34.7)	44.7 (13.5)	88.5 (81.8)	405 (508) [°]	396 (474) [°]	482 (325) [°]
MCV	0	178 (133) [†]	38.9 (9.7)	16.7 (1.1) ^{**°}	101 (57.7) ^{††}	34.3 (9.1) [°]	17.8 (1.1) ^{**°}
	60	234 (120)	49.7 (12.9)	55.2 (34.2) [°]	164 (150)	122 (110) [°]	82.3 (32.0) [°]
No. of experiments		5	5	6	6	8	6

Comparison of CD and CD-HAP samples: [†] $P < 0.05$; ^{††} $P < 0.01$
 Comparison of CD-HAP and CD-HAPdU samples: ^{*} $P < 0.05$; ^{**} $P < 0.01$
 Comparison of samples immediately and 60 min after evaporation: [°] $P < 0.05$

development of CaOx crystals as shown by X-ray crystallographic analysis of the precipitate. As illustrated in Table 1, a volume reduction to 70–80 ml and 40–50 ml increased the CaOx content in comparison with that recorded in the precipitate retrieved from the CD solution. Crystals of calcium oxalate monohydrate (COM) were almost entirely found in these samples, whereas, in the absence of HAP crystals, only COD was found. A more common occurrence of CaOx crystals in the CD-HAP solution compared with the CD solution was also demonstrated with SEM (Figs. 2C, 3C).

In sample B, the number of crystals was about twice as high in the CD-HAPdU solution compared with the CD-HAP solution, both immediately after evaporation and after 60 min ($P < 0.01$; Table 2). A much smaller and statistically insignificant difference between the two solutions was recorded in sample A. The total crystal volume was significantly higher in sample B from the

CD-HAPdU solution. These effects could be explained by a larger number of small crystals (Table 3). A significantly lower MCV in the CD-HAPdU solution was observed in both samples A and B immediately after evaporation ($P < 0.01$).

Scanning electron micrographs in Figs. 3C, D, 4C, D show that the crystals were smaller and apparently less aggregated in the CD-HAPdU solutions than in the CD-HAP solutions.

For the most extensively evaporated samples, which were reduced to a volume of 10–39 ml, there was no evident difference in terms of number of crystals, crystal volume or MCV compared with the CD-HAP solution. In the CD-HAPdU solution, however, there were a larger number of small crystals than in the CD-HAP solution. By SEM examination of the precipitate reduced to a volume of 10–20 ml it was also obvious that the crystals from the CD-HAPdU solutions were smaller than those from the CD-HAP solutions (Figs. 3E, 4E),

Table 3 Mean (SD) number and total crystal volume at different sample volumes immediately and 60 min after evaporation of 100 ml samples of CD, CD-HAP and CD-HAPdU-solutions

Crystal size interval (μm)	Time (min)	Sample A (70–95 ml)			Sample B (40–69 ml)		
		CD	CD-HAP	CD-HAPdU	CD	CD-HAP	CD-HAPdU
No. of crystals							
2.4–5.1	0	88 (92) ^{††}	1279 (371) [°]	1328 (444)	294 (289) ^{††°}	1670 (504)	3592 (1755)*
	60	94 (94)	840 (206) [°]	1198 (569)	1484 (1109) [°]	1833 (658)	3979 (1359)**
5.1–10.2	0	35 (32) [†]	79 (19)	142 (147) [°]	42 (45) ^{†°}	107 (47) [°]	290 (126)** [°]
	60	24 (36)	77 (34)	196 (190) [°]	340 (345) [°]	596 (523) [°]	1291 (981) [°]
10.2–20.2	0	7 (12)	5 (3.2)	8.2 (6.0)	11 (19) [°]	6.8 (5.0) [°]	12.3 (1.2) [°]
	60	7 (13)	7.8 (5.5)	20 (28)	164 (227) [°]	172 (288) [°]	125 (104) [°]
> 20.2	0	1 (1.4)	1 (0.7)	0.8 (1.0)	0.83 (0.9)	0.75 (0.9)	0.8 (0.8)
	60	2 (1.3)	0.6 (0.6)	0.5 (0.9)	85 (195)	3.3 (5.1)	3 (4.0)
Total crystal volume ($1000 \times \mu\text{m}^3$)							
2.4–5.1	0	2.2 (1.7) ^{††}	22.6 (7.8) [°]	24.8 (10.3)	5.5 (4.7) ^{††°}	29.9 (9.5)	70.4 (35.9) ^{*°}
	60	6.1 (2.8) ^{††}	15.9 (4.4) [°]	23.4 (12.3)	31.5 (24.6) [°]	41.6 (15.1)	99.4 (47.4) [°]
5.1–10.2	0	6.6 (6.5)	11.6 (3.1)	21.6 (22.9) [°]	8.2 (9.3) ^{†°}	17.1 (8.4) [°]	41.7 (18.1)** [°]
	60	6.3 (5.8)	12.3 (5.4)	35.1 (37.9) [°]	69.6 (75.1) [°]	219 (330) [°]	23.0 (17.1) [°]
10.2–20.2	0	8.3 (15.2)	6.3 (5.1)	9.8 (7.3)	12.7 (21.9) [°]	7.7 (5.4) [°]	14.8 (4.1) [°]
	60	9.6 (17.5)	10.2 (9.7)	22.1 (29.2)	233 (336) [°]	189 (335) [°]	133 (135) [°]
> 20.2	0	17.1 (20.7)	13.3 (13.8)	5.3 (6.0)	4.4 (5.5) [°]	11.1 (16.8)	6.9 (7.8)
	60	11.3 (10.0)	8.5 (9.3)	7.9 (16.9)	190 (377) [°]	23.1 (39.3)	20.8 (23.5)
No. of experiments		5	5	6	6	8	6

Comparison of CD and CD-HAP samples: [†] $P < 0.05$; ^{††} $P < 0.01$

Comparison of CD-HAP and CD-HAPdU samples: * $P < 0.05$; ** $P < 0.01$

Comparison of samples immediately and 60 min after evaporation: [°] $P < 0.05$

while no important difference was recorded between samples from CD solutions and CD-HAP solutions (Figs. 2E, 3E).

Ion-activity products

The ion-activity product of AP_{CaOx} exceeded the thermodynamic solubility product for CaOx (SP_{CaOx}) of $0.23\text{--}0.25 \times 10^{-8} \text{ M}^2$ [42, 55] in the samples already before evaporation. A formation product of CaOx (FP_{CaOx}) around $2 \times 10^{-8} \text{ M}^2$ was achieved already at a volume reduction to only 90 ml (Table 4). The solutions were supersaturated with respect to CaP , thus the AP_{OCP} and AP_{HAP} much exceeded the solubility product (SP) of $8.3 \times 10^{-48} \text{ M}^8$ for SP_{OCP} and of $2.35 \times 10^{-59} \text{ M}^9$ for SP_{HAP} [27] (Table 4). The AP_{Bru} exceeded the SP_{Bru} of $1.87 \times 10^{-7} \text{ M}^2$ in the non-evaporated solutions but an FP_{Bru} of $2 \times 10^{-6} \text{ M}^2$ [27, 38] was reached only after a volume reduction to 30 ml. It needs to be emphasized, however, that when the ion-activity products were calculated, the decrease in pH during volume reduction and complex binding between ions and urinary macromolecules were not accounted for. The ion-activity products, particularly, of different calcium phosphate salts might, therefore, be overestimated.

Discussion

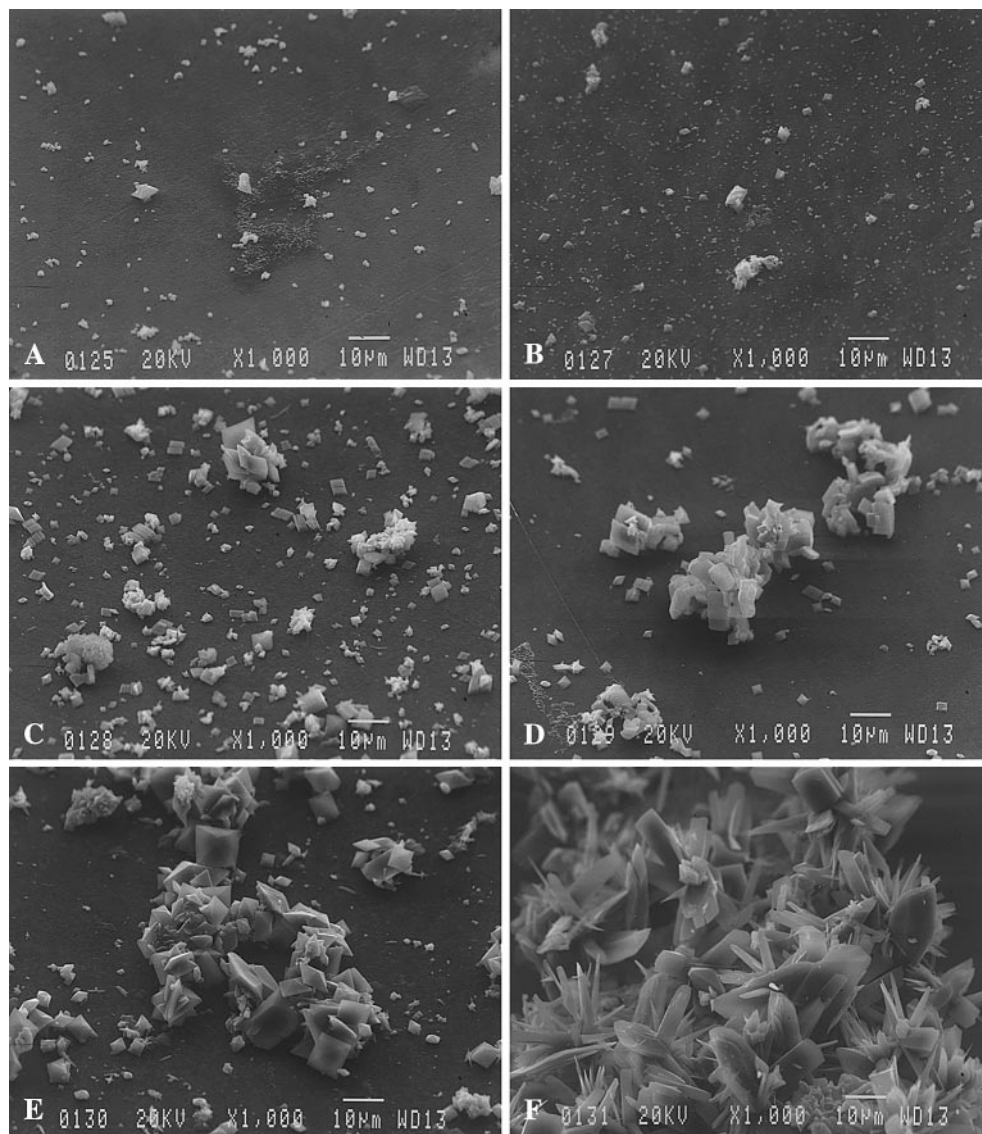
As shown in these experiments, addition of HAP crystals to a CD solution resulted in deposition of CaOx already

at a volume reduction of only 20–30%. This finding gives support to the hypothesis that CaP crystals formed at a nephron level above the collecting ducts [3, 12, 14, 18, 26, 34, 54] might promote the formation of a CaOx precipitate when these crystals encounter the urine environment in the collecting duct, at which level of the nephron both pH and urine volume are reduced.

Under normal conditions the pH will be around 6.75 in the proximal tubule and 6.45 in the distal tubule [48] and it has previously been shown in our laboratory that CaP is the type of crystal that most easily forms at these levels [53], whereas CaOx is the most likely product of crystallization in the collecting duct [18, 34]. According to measurements carried out by Asplin and coworkers [3] the pH and the risk of CaP precipitation might also be high in the loop of Henle. This crystallization risk depends, among others factors, on the phosphate concentration in the loop of Henle. In this respect it is noteworthy that stone formers have been shown to have an abnormally high phosphate excretion in response to a dietary load [49, 50].

Irrespective of the exact level of CaP precipitation in the nephron, the crystal material will probably move downwards in the nephron. Although small and unretained crystals will be eliminated with the urine, this will not be the case with crystals that are retained either because of their particle size or because of morphological abnormalities in the tubular layer of the collecting duct. Khan [24] has shown, for example, that crystals can easily get lodged in the distal part of the collecting duct where the channels bend. The interaction between crystals and cells that has been demonstrated by several

Fig. 3A–F Scanning electron microscopic examination of the precipitate after evaporation of 100 ml samples of CD-HAP solution. **A, B** Evaporated down to a final volume of 70–80 ml, **A** immediately after evaporation and **B** 60 min after evaporation. **C, D** Evaporated down to a final volume of 40–50 ml, **C** immediately after evaporation and **D** 60 min after evaporation. **E, F** Evaporated down to a final volume of 10–20 ml, **E** immediately after evaporation and **F** 60 min after evaporation. The precipitate is shown at a magnification of $\times 1000$



authors [8, 9, 11, 23, 32, 56] might be extremely important for the development of crystals formed in the nephron. It has been shown that CaP can bind to MDCK cells, which have characteristics of the cells in the distal tubule and the collecting duct. These adhesions resemble small microliths [37].

When retained CaP crystals are exposed to the low pH, they might dissolve either partially or completely. Although this dissolution obviously is counteracted by urinary macromolecules [19, 21, 54] it can nevertheless be sufficient to cause a local increment in the supersaturation with CaOx and hence CaOx nucleation [19, 21].

The effect of HAP was studied in both the presence and absence of dU. The presence of macromolecules resulted in a larger number of crystals and a reduced MCV. This most probably is caused by the inhibition of growth and aggregation of the CaP crystals [20]. Urinary macromolecules can also be expected to inhibit the heterogeneous nucleation of CaOx. In comparison with solutions without dU the content of CaOx that

precipitated following a small volume reduction was lower in solutions with dU. With the higher CaOx supersaturation following more extensive evaporation, this difference essentially disappeared. The exact mechanism behind this inhibition has not been elucidated, but it is reasonable to assume that liberated Ca^{2+} ions bind to γ -carboxylglutamic acid groups in the macromolecules [31, 39]. Such a binding would, thus, counteract the development of a local critical supersaturation when the solution supersaturation remains low, but not when it becomes high as a result of a pronounced volume reduction.

The increased number of small crystals that appeared following limited volume reduction of CD-HAP solutions was almost certainly the result of CaOx nucleation on CaP crystals previously below the detection limit of the Coulter counter. The increased fraction of CaP associated with extensive volume reductions in the form of brushite was an interesting and unexpected finding. It is reasonable to assume that this is explained

Fig. 4A–F Scanning electron microscopic examination of the precipitate after evaporation of 100 ml samples of CD-HAPdU solution. **A, B** Evaporated down to a final volume of 70–80 ml, **A** immediately after evaporation and **B** 60 min after evaporation. **C, D** Evaporated down to a final volume of 40–50 ml, **C** immediately after evaporation and **D** 60 min after evaporation. **E, F** Evaporated down to a final volume of 10–20 ml, **E** immediately after evaporation and **F** 60 min after evaporation. The precipitate is shown at a magnification of $\times 1000$

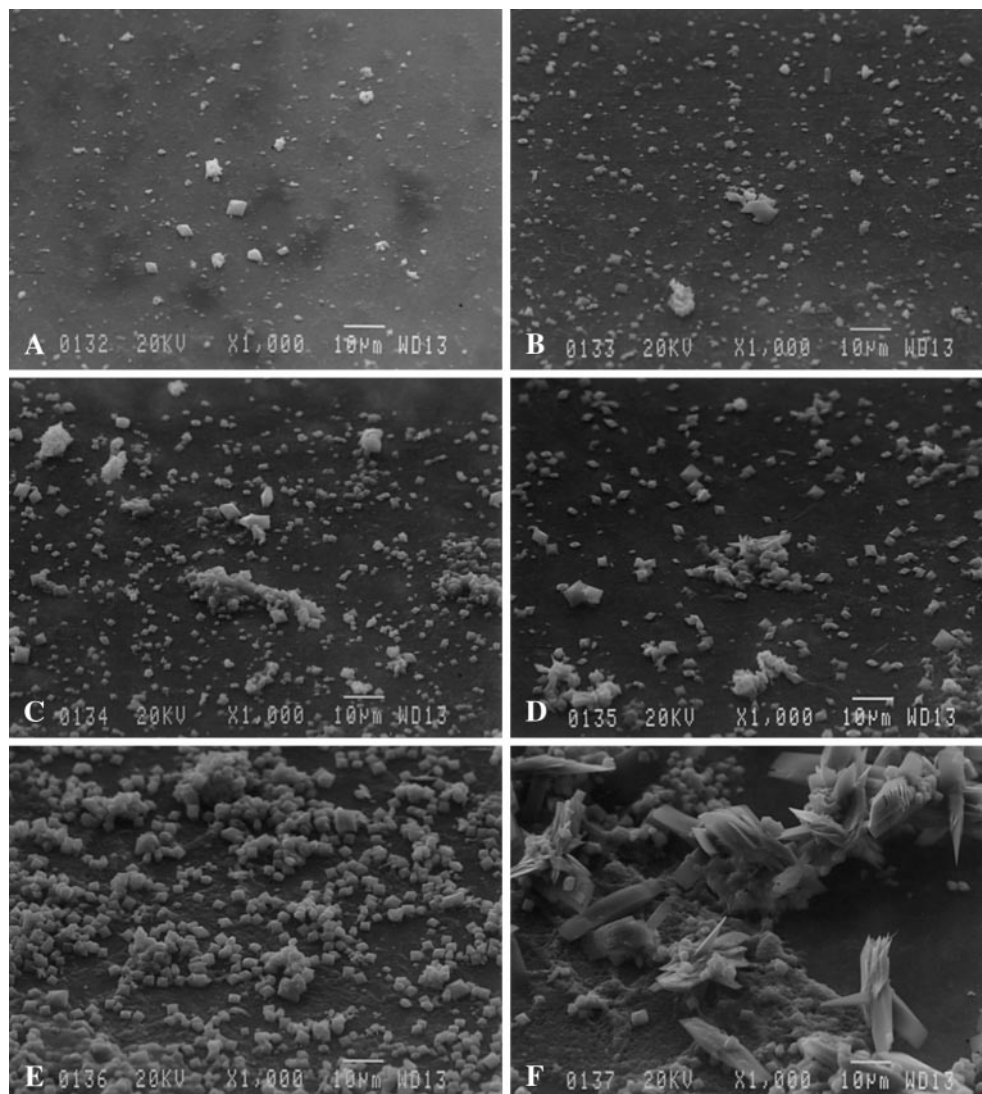


Table 4 Ion-activity products (AP) for calcium oxalate and different calcium phosphate salts at different volumes after evaporation of 100 ml of the CD solution (*CaOx* calcium oxalate, *ACP* amorphous calcium phosphate, *OCP* octacalcium phosphate, *HAP* hydroxyapatite, *Bru* brushite)

Volume after evaporation (ml)	$10^8 \times AP_{CaOx}$ (mol/l) ²	$10^{12} \times AP_{ACP}$ (mol/l) ²	$10^{25} \times AP_{OCP}$ (mol/l) ⁸	$10^{48} \times AP_{HAP}$ (mol/l) ⁹	$10^7 \times AP_{Bru}$ (mol/l) ²
100	1.94	1.82	1.60	0.74	4.59
90	2.18	1.83	2.03	1.56	5.32
80	2.43	1.86	2.67	3.54	6.28
70	2.78	1.90	3.59	8.51	7.56
60	3.20	1.98	5.08	22.5	9.38
50	3.86	2.13	7.57	65.0	12.1
40	4.82	2.43	12.2	204	16.7
30	6.43	3.15	21.9	645	25.1
20	9.55	5.59	45.7	1454	45.0
10	17.1	9.36	183	23 000	108

by a transformation of HAP to brushite in the acid environment [1, 33] and as a result of the increased calcium/magnesium ratio [1]. Obviously brushite most easily formed in the absence of both HAP seed and urinary macromolecules. The very high content of brushite that was recorded following volume reduction to 12–20 ml is unlikely under clinical conditions and

probably a volume reduction to 70–80 ml best reflects what happens in the urine of stone-formers.

The assessment of crystal formation with the Coulter counter technique is associated with several problems. Most importantly, as only crystals with a diameter greater than 2.4 μm were recorded, anything that happens in the smaller size range is not known. With this

shortcoming in mind we recorded the number and size distribution of crystals and derived an estimate of MCV. Although MCV is sensitive to variations in crystal number we nevertheless found MCV useful for approximately expressing the crystallization process. In this respect we paid no attention to the possible effect of an increased ion strength.

The presence of small HAP seeds apparently resulted in a controlled secondary nucleation, since both CD-HAP and CD-HAPdU solutions had an MCV smaller than that in the CD solutions, at least with the size distribution used in these experiments. A more heterogeneous size distribution with large CaP crystals or crystal aggregates would, in contrast, provide a basis for the formation of easily retained CaP/CaOx crystal masses.

In conclusion, we were able to demonstrate that volume reduction of solutions with a composition corresponding to that in the collecting duct resulted in precipitation of CaOx and that HAP crystals might augment such a process. The precipitation of CaOx was most obvious when limited volume reduction was carried out, similar to that expected under clinical conditions.

Acknowledgements We are grateful to Ms. Irène Ericsson for the assistance with the EQUIL2 calculations, and to Mr. Bengt-Arne Fredriksson for his unfailing help in the performance of scanning electron microscopy. The study was supported by grants from the Foundations of the Linköping Medical Society and Ake Wiberg, Sweden.

References

- Abbona F, Franchini-Angela M (1990) Crystallization of calcium and magnesium phosphates from solutions of low concentration. *J Crystal Growth* 104:661
- Achilles W, Jöckel U, Schaper A, Ulshöfer B, Riedmiller H (1994) Formation of urinary stones in vitro: growth of calcium oxalate on spherulites of calcium phosphate in gel. In: Ryall R, Bais R, Marshall VR, Rofe AM, Smith LH, Walker VR (eds) *Urolithiasis 2*. New York, Plenum Press, pp 161
- Asplin JR, Mandel NS, Coe FL (1996) Evidence for calcium phosphate supersaturation in the loop of Henle. *Am J Physiol* 270:F604
- Baumann JM, Futterlieb A, Lustenberger FX, Wacker M (1984) Crystallization phenomena in human urine after an alimentary oxalate load. In: Vahlensieck W, Gasser E (eds) *Fortschritte der Urologie und Nephrologie 22*. Steinkopff, Darmstadt, pp 151
- Baumann JM (1985) Invited review: Can the formation of calcium oxalate stones be explained by crystallization processes in urine *Urol Res* 13:267
- Baumann JM, Ackermann D, Affolter B (1989) The influence of hydroxyapatite and pyrophosphate on the formation product of calcium oxalate at different pH. *Urol Res* 17:153
- Berg C, Tiselius HG (1989) The effects of citrate on hydroxyapatite induced calcium oxalate crystallization and on the formation of calcium phosphate crystals. *Urol Res* 17:167
- Boevé ER, Ketelaars GAM, Vermeij M, Cao LC, Schröder H, de Bruijn WC (1993) An ultrastructural study of experimentally induced microlith in rat proximal and distal tubules. *J Urol* 149:893
- Boevé ER, Cao LC, Verkoelen CF, Romijn JC, de Bruijn WC, Schröder H (1994) Glycosaminoglycans and other sulfated polysaccharides in calculogenesis of urinary stones. *World J Urol* 12:43
- Boyce WH (1956) The amount and nature of the organic matrix in urinary calculi: a review. *J Urol* 76:213
- de Bruijn WC, Boevé ER, van Run PRWA, van Miert PPMC, Romijn JC, Verkoelen CF, Cao LC, Schröder FH (1994) Etiology of experimental calcium oxalate monohydrate nephrolithiasis in rats. *Scanning Microsc* 8:541
- Coe FL, Parks JH (1990) Defences of an unstable compromise: crystallization inhibitors and the kidney's role in mineral regulation. *Kidney Int* 38:625
- Christoffersen MR, Christoffersen J, Kibalczyk W (1990) Apparent solubilities of two amorphous calcium phosphates and of octacalcium phosphate in the temperature range 30 to 42°C. *J Crystal Growth* 106:349
- DeGanella S, Asplin J, Coe FL (1990) Evidence that tubule fluid in the thin segment of the loop of Henle normally is supersaturated and forms a poorly crystallized hydroxyapatite that can initiate renal stones. *Kidney Int* 37:472
- Finlayson B, Reid F (1978) The expectation of free and fixed particles in urinary stone disease. *Invest Urol* 15:442
- Grases F, Conte A (1992) Urolithiasis, inhibitors and promoters. *Urol Res* 20:86
- Hallson PC, Rose GA (1989) Measurement of calcium phosphate crystalluria: influence of pH and osmolality and invariable presence of oxalate. *Br J Urol* 64:458
- Højgaard I, Fornander AM, Nilsson MA, Tiselius HG (1996) Crystallization during volume reduction of solutions with an ion-composition corresponding to that in the distal tubuli. *Scanning Microsc* 10:487
- Højgaard I, Fornander AM, Nilsson MA, Tiselius HG (1998) The effect of pH change on the crystallization of calcium salts in solutions with an ion composition corresponding to that in the distal tubule. *Urol Res*, in press
- Højgaard I, Tiselius HG (1998) The effects of citrate and urinary macromolecules on the aggregation of hydroxyapatite crystals in solutions with a composition similar to that in the distal tubule. *Urol Res* 26:89
- Højgaard I, Fornander AM, Nilsson MA, Tiselius HG (1998) The influence of hydroxyapatite seed on the crystallization induced by volume reduction of solutions with an ion-composition corresponding to that in the distal tubule at different pH levels. *Scand J Urol Nephrol* 32:311
- Hufnagel A, Ottenjann H, Scaper A, Achilles W (1995) Experiments on the formation of artificial urinary stones. I. Effects of spherulites of calcium phosphate on the morphology of stone-like particles. In: Tiselius HG (ed) *Renal stones: aspects on their formation, removal and prevention*. Proceedings of the Sixth European Symposium on Urolithiasis, Stockholm, Sweden, p 30
- Khan SR, Hackett RL (1991) Retention of calcium oxalate crystals in renal tubules. *Scanning Microsc* 5:707
- Khan SR (1995) Calcium oxalate crystal interaction with renal tubular epithelium, mechanism of crystal adhesion and its impact on stone development. *Urol Res* 23:71
- Kok DJ, Khan SR (1994) Calcium oxalate nephrolithiasis, a free or fixed particle disease. *Kidney Int* 46:847
- Kok DJ (1995) Intratubular crystallization events. In: Tiselius HG (eds) *Renal stones: aspects on their formation, removal and prevention*. Proceedings of the Sixth European Symposium on Urolithiasis, Stockholm, pp 26
- Koutsoukos PG, Nancollas GH (1981) Crystal growth of calcium phosphates: epitaxial considerations. *J Crystal Growth* 53:10
- Larsson L, Öhman S, Sörbo B, Tiselius HG (1984) Wet chemical analysis of small (<20 mg) urinary calculi. In: Ryall R, Brochis JG, Marshall V, Finlayson B (eds) *Urinary stone*. Churchill Livingstone, London, pp 339
- Larsson L, Öhman S, Sörbo B, Tiselius HG (1984) A method for quantitative analysis of urinary calculi. *Clin Chim Acta* 140:9
- Leusmann DB, Entrup M, Schmandt W, Blaschke R (1984) Results of the combined phase and texture analyses of 1028 urinary concrements. *Urol Res* 12:94

31. Lian JB, Prien ELJ, Glimcher MJ, Gallop PM (1977) The presence of protein bound gamma-carboxyglutamic acid in calcium containing renal calculi. *J Clin Invest* 59:1151
32. Lieske JC, Toback FG (1993) Regulation of renal epithelial cell endocytosis of calcium oxalate monohydrate crystals. *Am J Physiol* 264:F800
33. Lundager-Madsen HE, Christensson F (1991) Precipitation of calcium phosphate at 40°C from neutral solution. *J Crystal Growth* 114:613
34. Lupták J, Jensen HB, Fornander AM, Højgaard I, Nilsson MA, Tiselius HG (1994) Crystallization of calcium oxalate and calcium phosphate at supersaturation levels corresponding to those in different parts of the nephron. *Scanning Microsc* 8:47
35. Meyer JL, Bergert JH, Smith LH (1975) Epitaxial relationships in urolithiasis: the calcium oxalate monohydrate-hydroxyapatite system. *Clin Sci Mol Med* 49:369
36. Meyer JL, Bergert JH, Smith LH (1977) Epitaxial relationships in urolithiasis: the brushite-whewellite system. *Clin Sci Mol Med* 52:143
37. Naito Y, Ohtawara Y, Kageyama S, Nakano M, Ichiyama A, Fujita M, Suzuki K, Kawabe K, Kino I (1997) Morphological analysis of renal cell culture models of calcium phosphate stone formation. *Urol Res* 25:59
38. Nancollas GH (1982) Phase transformation during precipitation of calcium salts. In: Nancollas GH (ed) *Biological mineralization and demineralization*. Springer, Berlin, p 79
39. Nishio S, Kavanagh JP, Fargher EB, Garside J, Blacklock NJ (1990) Calcium oxalate crystallization kinetics and the effects of calcium and gamma-carboxyglutamic acid. *Br J Urol* 66:351
40. Ohkawa M, Tokunaga S, Nakashima T, Yamaguchi K, Orito M, Hisazumi H (1992) Composition of urinary calculi related to urinary tract infection. *J Urol* 148:995
41. Pak CYC, Eanes ED, Ruskin B (1971) Spontaneous precipitation of brushite in urine: evidence that brushite is the nidus of renal stones originating as calcium phosphate. *Proc Natl Acad Sci USA* 68:1456
42. Pak CYC, Ohata M, Holt K (1975) Effect of diphosphonate on crystallization of calcium oxalate in vitro. *Kidney Int* 7:154
43. Pak CYC, Hayashi Y, Arnold LH (1976) Heterogenous nucleation with urate, calcium phosphate and calcium oxalate. *Proc Soc Exp Biol Med* 153:83
44. Pak CYC (1981) Potential etiologic role of brushite in the formation of calcium (renal) stones. *J Crystal Growth* 53:202
45. Peacock M, Robertson WG, Marshall RW (1979) Disorders associated with renal calcium-stone disease. *Endocrinology* 2:823
46. Prien L (1955) Studies in urolithiasis. III. Physicochemical principles in stone formation and prevention. *J Urol* 73:627
47. Prien L Sr (1975) The riddle of Randall's plaques. *J Urol* 114:500
48. Rector FC Jr (1983) Acidification of the urine. In: Geiger SR, Orloff J, Berliner RW (eds) *Renal physiology*, section 8, *Handbook of physiology*. American Physiological Society, Washington, DC, p 431
49. Schwille PO, Schmiedl A, Herrmann U, Wipplinger J (1997) Postprandial hyperinsulinaemia, insulin resistance and inappropriately high phosphaturia are features of younger males with idiopathic urolithiasis: attenuation by ascorbic acid supplementation of a test meal. *Urol Res* 25:49
50. Schwille PO, Herrmann U, Schmiedl A, Kissler H, Wipplinger J, Manoharan M (1997) Urinary phosphate excretion in the pathophysiology of idiopathic recurrent calcium urolithiasis: hormonal interactions and lipid metabolism. *Urol Res* 25:417
51. Smith LH, Werness PG (1983) Hydroxyapatite: the forgotten crystal in calcium urolithiasis. *Trans Am Clin Chem Assoc* 95:183
52. Tiselius HG (1996) Solution chemistry of supersaturation. In: Coe FL, Favus MJ, Pak CYC, Parks JM, Preminger GM (eds) *Kidney stones: medical and surgical management*. Lippincott-Raven, Philadelphia, pp 33
53. Tiselius HG, Fornander AM, Nilsson MA (1997) Estimated levels of supersaturation with calcium phosphate and calcium oxalate in the distal tubule. *Urol Res* 25:153
54. Tiselius HG, Fornander AM, Nilsson MA (1998) Studies on the crystallization process following addition of calcium phosphate crystals to solutions with a composition corresponding to that in the collecting duct. *Scanning Microsc*, in press
55. Tomazic B, Nancollas GH (1979) The kinetics of dissolution of calcium oxalate hydrates. *J Crystal Growth* 46:355
56. Verkoelen CF, Romijn JC, Cao LC, Boevé ER, de Bruijn WC, Schröder FH (1996) Crystal-cell interaction inhibition by polysaccharides. *J Urol* 155:749
57. Werness PG, Brown CM, Smith LH, Finlayson B (1985) EQUIL2: basic computer program for the calculation of urinary saturation. *J Urol* 134:1242